Phosphorus transformations along a large-scale climosequence in arid and semi-arid grasslands of northern China

Jiao Feng[1,2], Benjamin L. Turner[3], Xiaotao Lü[1], Zhenhua Chen[1], Kai Wei[1], Jihui Tian[1,2], Chao Wang[1,2], Wentao Luo[1,2], and Lijun Chen[1]

[1] Institute of Applied Ecology, Chinese Academy of Sciences, Shenyang 110016, China.

[2]University of Chinese Academy of Sciences, Beijing 100049, China.

[3]Smithsonian Tropical Research Institute, Apartado 0843-03092, Balboa, Ancon, Republic of Panama.

Corresponding author: Lijun Chen (ljchenchina@hotmail.com; ljchen@iae.ac.cn)
Institute of Applied Ecology, Chinese Academy of Sciences

Institute of Applied Ecology
Chinese Academy of Sciences
P. O. Box 417
Shenyang 110016
China
Telephone: +86-24-83970355
Fax: +86-24-83970300

Key Points:

- Decreasing aridity in drylands has a similar effect on soil phosphorus transformations as time
- The Walker and Syers model can be extended to dryland climosequences
- Pedogenic and biogeochemical changes occur at an aridity threshold of about 0.7

This article has been accepted for publication and undergone full peer review but has not been through the copyediting, typesetting, pagination and proofreading process which may lead to differences between this version and the Version of Record. Please cite this article as doi: 10.1002/2015GB005331

Abstract

The Walker and Syers model of phosphorus (P) transformations during long-term soil development has been verified along many chronosequences, but has rarely been examined along climosequences, particularly in arid regions. We hypothesized that decreasing aridity would have similar effects on soil P transformations as time by increasing the rate of pedogenesis. To assess this, we examined P fractions in arid and semi-arid grassland soils along a 3,700 km aridity gradient in northern China (aridity between 0.43 and 0.97, calculated as 1–[mean annual precipitation / potential evapotranspiration]). Primary mineral P declined as aridity decreased, although it still accounted for about 30% of the total P in the wettest sites. In contrast, the proportions of organic and occluded P increased as aridity decreased. These changes in soil P composition occurred in parallel with marked shifts in soil nutrient stoichiometry, with organic carbon:organic P and nitrogen:organic P ratios increasing with decreasing aridity. These results indicate increasing P demand relative to carbon or nitrogen along the climosequence. Overall, our results indicate a broad shift from abiotic to biotic control on P cycling at an aridity threshold of approximately 0.7 (corresponding to about 250 mm mean annual rainfall). We conclude that the Walker and Syers model can be extended to climosequences in arid and semi-arid ecosystems, and that the apparent decoupling of nutrient cycles in arid soils is a consequence of their pedogenic immaturity.

1 Introduction

Phosphorus (P) is one of the most important elements in biological systems, because it commonly limits terrestrial ecosystem production [*Craine et al.*, 2008; *Vitousek et al.*, 2010] and regulates key ecological processes such as soil organic matter (SOM) accumulation, nitrogen (N) fixation and carbon (C) stabilization [*Walker and Adams*, 1958; *Mackenzie et al.*, 2002; *Vitousek et al.*, 2010]. In nature, soil P is derived almost entirely from geochemical weathering of parent material [*Lajtha and Schlesinger*, 1988], with relatively small inputs from eolian deposition [*Okin et al.*, 2004; *Selmants and Hart*, 2010]. Plants and microbes incorporate P into biomass and return it to the soil in organic forms, which can then be recycled by phosphatase enzymes to release inorganic phosphate for biological uptake [*Walker and Syers*, 1976; *Cross and Schlesinger*, 1995; *Turner et al.*, 2007]. The P cycle is therefore regulated by both geochemical and biological processes [*Cross and Schlesinger*, 2001; *Delgado-Baquerizo et al.*, 2013]. Identifying and quantifying the transformations and pools of soil P can provide insight into the abiotic and biotic controls on the availability of this essential nutrient [*Cross and Schlesinger*, 2001; *Delgado-Baquerizo et al.*, 2013].

The amount and chemical composition of soil P are related to pedogenesis [*Walker*, 1965; *Walker and Syers*, 1976; *Lajtha and Schlesinger*, 1988; *Turner et al.*, 2007; *Yang and Post*, 2011]. Based on four soil chronosequences developed in contrasting climates and ecosystems in New Zealand, Walker and Syers [1976] proposed a general model to predict the dynamics of P during long-term pedogenesis. Phosphorus released from primary minerals by weathering can become sorbed to soil particles, lost from the soil profile in leachate, or assimilated by biomass and enter the organic P (P_o) pool. Over longer timescales, P can become associated with secondary minerals such as aluminum (Al) and iron (Fe) oxides and transformed into stable forms known collectively as occluded P. In old soils on stable land surfaces, a "terminal steady state" is reached, whereby primary mineral P is exhausted, the

total P concentration is low, P input from dust deposition is of similar magnitude to P export in runoff, and the remaining soil P is predominantly in organic and occluded inorganic forms [*Walker and Syers*, 1976].

Compared to soils in more humid regions, arid soils typically contain little SOM, and carbonate minerals are the predominant reservoir of P [*Lajtha and Schlesinger*, 1988; *Cross and Schlesinger*, 1995]. This is due mainly to reduced water inputs in arid environments, which limits leaching and allows calcium (Ca) minerals to accumulate [*Lajtha and Schlesinger*, 1988; *Ippolito et al.*, 2010]. In addition, little P is incorporated into biomass because of water limitation, leading to a small P_o pool in arid soils [*Lajtha and Schlesinger*, 1988; *Delgado-Baquerizo et al.*, 2013]. Weathering of primary minerals is thus more important than biological mineralization of P_o in supplying P to plants in arid soils [*Delgado-Baquerizo et al.*, 2013]. In humid soils, however, a greater proportion of the P occurs in organic compounds or bound to secondary Al and Fe oxides, which can reduce P availability to plants and microbes [*Walker and Syers*, 1976; *Cross and Schlesinger*, 1995; *McGroddy et al.*, 2008]. Biological mineralization of P_o is therefore essential to maintain the bioavailable P pool in humid sites [*Walker and Syers*, 1976; *Crews et al.*, 1995; *Izquierdo et al.*, 2013]. These differences could cause the biogeochemical transformations and availability of P to differ fundamentally between arid and humid soils [*Cross and Schlesinger*, 1995; *Ippolito et al.*, 2010].

Walker and Syers [1976] suggested that, compared to humid sites, it would take longer for soil P transformations to occur in arid sites with low leaching intensity. They were therefore careful to predict that their model would apply only to soils formed under humid ecosystems on stable land surfaces [*Walker and Syers*, 1976; *Turner and Condron*, 2013]. The Walker and Syers model has since been validated along a number of chronosequences in humid ecosystems [*Tiessen et al.*, 1984; *Crews et al.*, 1995; *Vitousek and Farrington*, 1997;

Richardson et al., 2004; *Izquierdo et al.*, 2013], yet only a few studies have been conducted in more arid ecosystems [*Lajtha and Schlesinger*, 1988; *Selmants and Hart*, 2010; *Turner and Laliberté*, 2015]. Lajtha and Schlesinger [1988] observed little transformation of P from Ca-bound forms to Fe- and Al-bound forms even in the oldest soils of an arid chronsosequence (25,660 yr BP), which they attributed to the low weathering intensity. However, Selmants and Hart [2010] observed decreasing primary mineral P and increasing P_o across a three million year volcanic chronosequence in northern Arizona, USA, demonstrating that the Walker and Syers model can also apply to soils under (modern) arid climates. These results highlight the uncertainty in applying the Walker and Syers model to ecosystem development under arid and semi-arid climates.

Walker and Syers [1976] proposed that soil development sequences consisted of soils arranged in order of enhanced development (weathering) brought about by greater age, greater precipitation, or decreasing slope. They suggested that pedogenesis was determined by the quantity of water leached through the soil profile, irrespective of whether this was driven by increasing soil age at constant precipitation, or by increasing precipitation in soils of the same age [*Walker and Syers*, 1976]. They observed substantial transformations of soil P with pedogenesis across several soil sequences in New Zealand, including chrono-, topo-, and hydrosequences [*Walker and Syers*, 1976]. Although particular emphasis has been placed subsequently on P transformations along soil chronosequences [*Crews et al.*, 1995; *Turner et al.*, 2007; *Selmants and Hart*, 2010; *Turner and Condron*, 2013; *Chen et al.*, 2015; *Turner and Laliberté*, 2015], relatively few studies have examined climosequences [*Ippolito et al.*, 2010; *Emadi et al.*, 2012] or toposequences [*Roberts et al.*, 1985; *Agbenin and Tiessen*, 1995].

In drier ecosystems, water availability is the critical determinant of the rate of weathering and pedogenesis, and often drives substantial changes in soil physical and chemical characteristics [*Ippolito et al.*, 2010; *Khormali and Kehl*, 2011; *Quénard et al.*, 2011]. Delgado- Baquerizo et al. [2013] argued that C, N and P cycles became decoupled with increasing aridity (manifested as decreases in soil C:P and N:P ratios), which they attributed to differences in the response of P to increasing aridity compared to the responses of C and N. Wardle [2013] commented that these decoupled nutrient cycles with increasing aridity operated in the opposite direction of ecosystem development. It could be argued therefore that climate might have similar effects on soil genesis and P cycling as time, with wetter soils equating to older soils in terms of greater P loss, wider C:P ratios, and stronger P limitation of biological processes [*Walker and Syers*, 1976; *Crews et al.*, 1995; *Selmants and Hart*, 2010; *Chen et al.*, 2015; *Turner and Laliberté*, 2015]. Consistent with this, Ippolito et al. [2010] observed a distinct decrease in Ca-bound P and an increase in occluded P with increasing precipitation across the central Great Plains in the USA, indicating the strong effect of precipitation on pedogenesis and P transformations in drier ecosystems.

We collected soil from 52 sites along a 3,700 km grassland transect in northern China. The transect is considered to represent a climate gradient and has been used to study how climate influences above- and belowground ecological processes and predict their responses to global climate change [*Zhou et al.*, 2002; *Wang et al.*, 2014; *Luo et al.*, 2015]. The transect provides an opportunity to investigate large-scale climate-driven P transformations in drylands. Increased aridity is predicted in global drylands [*Gao and Giorgi*, 2008; *Feng and Fu*, 2013], so patterns of P chemistry along the climosequence can inform our understanding and ultimately our ability to predict how biogeochemical P cycling will be affected by climate change.

We aimed to (1) identify and quantify soil P fractions in arid and semi-arid ecosystems across the climosequence, (2) assess the relative importance of abiotic and biotic controls on P availability in these drylands, and (3) test whether soil P transformations along the climosequence are consistent with the predictions of the Walker and Syers [1976] model, and are comparable to the patterns of soil P transformations along humid soil chronosequences.

2 Materials and Methods

2.1 Study sites

The study was conducted along a 3,700 km west-to-east transect across Xinjiang, Gansu province and Inner Mongolia, primarily on the Inner Mongolian Plateau (Figure 1). Elevation declines from about 1,200 m in the west to approximately 600 m in the east. However, the topography is muted, with tablelands and gently rolling hills [*Luo et al.*, 2016], allowing us to eliminate this soil forming factor as a major driver of pedogenesis along the climate gradient. The mean annual precipitation (MAP) increased from 34 mm in the west to 436 mm in the east, with 77%–98% (mean 88%) of the precipitation occurring between June and September. The mean annual temperature (MAT) varied from about 10 °C in the western sites to −3 °C in the eastern sites. The monthly mean temperature was below 0 °C in winter and early spring (between November and March) at all sites along the transect. The highest temperature occurred between June and August, with monthly mean temperature between 25 °C and 15 °C (mean 20 °C) from west to east along the transect. Annual potential evapotranspiration (PET) declined from about 1200 mm in the west to about 710 mm in the east. MAT was negatively correlated with MAP along the transect (R^2=0.889, P<0.001, Fig. S1). By including both MAP and MAT, the aridity measure provides an integrated index of

variation of climate [Equation 1, *Arora*, 2002], with aridity correlating negatively with MAP (R^2=0.992, P<0.001) and positively with MAT (R^2=0.898, P<0.001, Fig. S1).

$$\text{Aridity} = 1 - \frac{\text{MAP}}{\text{PET}} \qquad \text{Equation 1}$$

In the western sites, high temperature (high PET) coupled with low precipitation results in an extremely arid climate. In the eastern sites, low temperature (low PET) and high precipitation together alleviate the aridity. From west to east, aridity declines from 0.97 to 0.43 along the transect, indicating decreasing aridity and increasing humidity. Following this aridity gradient from dry (west; low precipitation, high temperature and PET) to wet (east; high precipitation, low temperature and PET), ecosystem type shifts gradually from arid grassland to semi-arid grassland, and the dominant vegetation types are desert shrub, desert steppe, typical steppe followed by meadow steppe (Figure 1).

Soils along the transect began forming during the Holocene [*Liangwu and Angjiang*, 2001; *Feng et al.*, 2006] and are therefore relatively weakly developed, with high concentrations of calcareous sediments close to the soil surface [*Irwin-Williams and Haynes*, 1970; *Feng et al.*, 2006]. The soils are formed primarily from loess deposits, although some have formed in diluvial and alluvial deposits and desert soils in the western sites can also receive eolian sands. Soils varied with decreasing aridity from Haplic Calcisols in the drier sites, to Calcic Cambisols at intermediate rainfall, and then Calcic Kastanozems at the wetter sites (Fig. 1). Haplic Calcisols are characterized by calcium carbonate accumulation at the soil surface and lack a calcic horizon (Bk), and are therefore in an initial stage of soil formation. Calcic Cambisols have minimal B-horizon development, and are considered to be in an intermediate stage of development [*FAO*, 1993]. Calcic Kastanozems are relatively mature soils with well-developed soil profiles, with secondary (pedogenic) carbonate accumulation at depth (i.e. with calcic horizons) [*FAO*, 1993]. Thus, the CaO content of surface soils along the transect declines from about 7% in Haplic Calcisols, to 3% in Calcic

Cambisols, and then 1% in Calcic Kastanozems [*Lei et al.*, 1990; *Shi et al.*, 1990], but has accumulated in subsurface horizons in Calcic Cambisols (20-50 cm) and Calcic Kastanozems (> 40 cm deep) [*Lei et al.*, 1990; *Shi et al.*, 1990].

All soils across the transect are sands or sandy loams, with >60% sand and a strong acid reaction [Fig. S2, *Wang et al.*, 2014; *Wang et al.*, 2016]. The mineral composition is similar in all three soil classes, with elemental composition after ignition dominated by SiO_2 (70–76%), with smaller amounts of Al_2O_3 (11–12%) and Fe_2O_3 (3–4%) [*Lei et al.*, 1990; *Shi et al.*, 1990]. This demonstrates that the parent loess is relatively homogenous across the transect.

Fifty-two sites were sampled at 50~100 km intervals along the climosequence during July-August, 2012. The geographical location and elevation of each site were recorded by Global Positioning Satellite device (eTrex Venture, Garmin, USA). At each site, five 1 m × 1 m sub-plots were selected within a 50 m × 50 m plot. In each sub-plot, all grasses were harvested for calculation of above ground primary production (ANPP). In a 5 m × 5 m sub-plot with shrubby vegetation, one fourth of annual branches were clipped to measure ANPP (expressed at per m^2). Three soil samples were collected using a 100 cm^3 cylinder (5 cm height × 5 cm diameter) to determine soil bulk density, and then twenty soil cores (0-10 cm depth, 2.5 cm diameter) were collected at random and homogenized. Stones and visible roots were removed in-situ, soils were sieved (< 2 mm) and stored in plastic bags. A subsample was stored at 4°C in the field and then frozen at −20°C upon return to the laboratory for biological analyses. A second subsample was immediately air-dried after sampling for the determination of abiotic properties. More detailed descriptions of the study region and sampling protocol can be found in Wang et al. [2014] and Luo et al. [2015].

2.2 Determination of soil total, inorganic, and organic phosphorus

Total P (P_t) was determine by igniting soil in a muffle furnace at 550 °C for 1 h [*Aspila et al.*, 1976]. A second subsample of unignited soil was used to determine the total inorganic P (P_i) concentration. Both ignited and unignited samples were shaken in 1 M H_2SO_4 for 16 h at 25 °C in a 1:30 soil to solution ratio and filtered through a 30-50 μm cellulose-nitrate membrane filter (ASTME832-81). Phosphate was determined at 880 nm by molybdate colorimetry on a spectrophotometer (Carry 500, Varian Company, USA). Soil P_o was estimated as the difference in P in ignited and unignited samples. This procedure can underestimate P_t in strongly weathered soils, but is generally appropriate for weakly and moderately weathered soils such as those along our climosequence [*Hance and Anderson*, 1962; *Williams et al.*, 1970].

2.3 Sequential phosphorus fractionation

Phosphorus fractions were extracted by a modified sequential Hedley fractionation scheme [*Tiessen and Moir*, 1993]. First, resin P was determined by shaking 1.000 g soil (dry weight) with 30 ml of deionized water and a clean anion-exchange resin strip (2.5 × 1 cm, 551642S, BDH-Prolabo, VWR International, Lutterworth, UK) in a 50 ml plastic centrifuge tube for 16 h at 25 °C in an overhead-shaker. Phosphorus retained on the resin strip was eluted by shaking the resin strip with 10 ml 0.25 M H_2SO_4 for 1 h. The soil sample was centrifuged at 8180 × *g* for 10 min, the supernatant decanted, and the remaining soil was shaken with 30 ml of 0.5 M $NaHCO_3$ (pH = 8.5) for 16 h at 25 °C ($NaHCO_3$-P). Using the same procedure, the remaining sample was then sequentially extracted with 0.1 M NaOH and 1 M HCl to extract NaOH-P and HCl-P, respectively. The hot HCl extraction step, introduced by Tiessen and Moir [1993] for strongly weathered tropical soils, was not included because the calcic soils in this study do not contain significant proportions of recalcitrant P associated

with secondary minerals. Finally, the residue was ignited in a muffle furnace at 550 °C for 1 h to determine residual P. Aliquots of the $NaHCO_3$, NaOH, and HCl extracts were digested with $K_2S_2O_8$-H_2SO_4 to determine P_t in the extracts, with P_o calculated as the difference between P_t and P_i. All extracts were determined by molybdate colorimetry at 880 nm on a spectrophotometer (Carry 500, Varian Company, USA). Available-P_i was the sum of resin-P and $NaHCO_3$-P_i; total P_i was the sum of resin-P, $NaHCO_3$-P_i, NaOH-P_i and HCl-P_i; total extracted P_o was the sum of $NaHCO_3$-P_o, NaOH-P_o and HCl-P_o; P_t was the sum of P_i and P_o. For comparison with the Walker and Syers [1976] model, the sequential P fractions were grouped into P_{Ca} (HCl- P_i), occluded P (residual-P), non-occluded P (sum of resin-P, $NaHCO_3$-P_i and NaOH-P_i) and P_o (sum of $NaHCO_3$-P_o, NaOH-P_o and HCl-P_o).

2.4 Climate data

Mean annual temperature, MAP and PET for each sampling site was extracted from the WorldClim data set using ArcGIS version 9.3 (Esri, Redlands, CA).

2.5 Statistical analysis

Pearson correlation analysis was carried out to quantify relationships between key soil chemical properties and concentrations of P fractions (SPSS 16.0, Benelux BV, Gorinchem, The Netherlands). Regression analyses were used to fit linear and polynomial data using Origin 9.0 software (OriginLab Corp., Northampton, MA, USA). Ordinary least squares (OLS) polynomial fitting was used to examine the relationships of aridity with soil P_t, P_o and P_i, and with soil P fractions as well. Ordinary least squares linear fitting was used to analyze the relationships between aridity and elemental ratios of soil C, N and P.

3 Results

3.1 Soil phosphorus fractions and soil elemental ratios across the aridity gradient

Soil P_t decreased from about 500 mg P kg^{-1} to about 300 mg P kg^{-1} in drier sites (aridity>0.70), followed by an increase to around 600 mg P kg^{-1} in wetter sites (aridity<0.70; Fig. 2a). Soil P_i declined, while P_o increased continuously along the climosequence from dry to wet (Fig. 2b, c). Soil P_o was correlated negatively with MAT (R^2=0.659, P<0.001, Fig. S3), but positively with MAP (R^2=0.805, P<0.001, Fig. S3). Soil organic C (SOC):P_o, N:P_o, SOC:P_t and N:P_t ratios were all correlated negatively with aridity (Fig. 3).

Non-occluded P_i (sum of resin-P, $NaHCO_3$-P_i and NaOH-P_i) accounted for < 14% of P_t (average 7%, 6 to 70 mg P kg^{-1}) (Fig. 4a; Fig. S4). This pool decreased initially and then increased across the aridity gradient from dry to wet, with the minimum value at aridity approximately 0.70 (Fig. 4a). The P_{Ca} (HCl-P_i) varied between 23 and 562 mg P kg^{-1} and accounted for the largest proportion of P_t (18–87%, mean 60%). The P_{Ca} concentration generally declined across the aridity gradient from dry to wet (Fig. 4b). Soil extracted P_o (the sum of $NaHCO_3$-P_o, NaOH-P_o and HCl-P_o) varied between 17 and 165 mg P kg^{-1} (4–55% of P_t, mean 19%) and increased progressively across the aridity gradient from dry to wet, with a slight increase in drier sites but a marked accumulation in wetter sites (Fig. 4c). The concentration of NaOH-P_o ranged from 2 to 130 mg P kg^{-1} (33 mg P kg^{-1} on average), and constituted on average 73% of total extractable P_o. $NaHCO_3$-P_o (0–20 mg P kg^{-1}) and HCl-P_o (0–45 mg P kg^{-1}) accounted for 12% and 15% of total extractable P_o on average, respectively (Fig. S4). Occluded-P (residual P, the most tightly bound P pool) accounted for 14% of P_t on average (0 to 129 mg P kg^{-1}, 0 to 34% of P_t), and progressively increased across the aridity gradient from dry to wet (Fig. 4d).

Changes in soil P pools along the climosequence are plotted in the same manner as the original Walker and Syers [1976] diagram of P transformations with time (Fig. 5). The concentration and proportion of P_{Ca} declined, while that of occluded P and extracted P_o increased with soil development (i.e. as a function of declining aridity) (Fig. 5). Soil P_t, calculated by the sum of all fractions (112–684 mg P kg^{-1}), did not decline significantly across the climosequence. There was an initial decrease in P_t in drier sites followed by an almost equal increase in wetter sites (Fig. 5a).

3.2 Relationship between soil total phosphorus determined by different methods

Soil P_t determined by sequential extraction (i.e. the sum of extracted P_i, P_o and residual P, Fig. 5) was correlated strongly with an independent measure of P_t determined by the ignition procedure (R^2= 0.775, P<0.01, n=52). Generally, P_t by sequential extraction was approximately 18% ± 8% less than P_t determined by ignition. This is likely due to systematic errors in the sequential fractionation method [*Tiessen and Moir*, 1993]. Overall, the values of P_t by different methods were comparable in these arid and semi-arid grassland ecosystems.

3.3 Relationships between soil chemical properties and phosphorus fractions

Extracted P_i and the dominant P_i fraction (HCl-P_i) were correlated positively with soil pH and soil exchangeable Ca, with Pearson product-moment correlation coefficients (r) between 0.535 and 0.651 (p<0.05, Table 1). Conversely, total extracted P_o, NaOH-P_i, and NaOH-P_o were correlated negatively with soil pH (r from –0.631 to –0.861, p<0.01) and soil exchangeable Ca (r from –0.337 to –0.348, $p<0.05$). Soil available-P_i, NaOH-P_i, NaOH-P_o and residual-P were correlated positively with both soil exchangeable Fe (r from 0.487 to 0.855, p<0.01) and Mn (r from 0.488 to 0.905, p<0.01).

4 Discussion

Changes in the concentrations and proportions of P_{Ca}, P_o, and occluded P along our climosequence are consistent with expectations of changes in soil P fractions during pedogenesis [*Walker and Syers*, 1976]. Based on a series of soil sequences in New Zealand, Walker and Syers suggested that pedogenesis depended predominantly on the volume of water leached through soil, irrespective of whether this occurred through increasing soil age at constant water availability or by increasing water availability in soils of the same age [*Walker and Syers*, 1976]. The strong redistribution of P from primary minerals to P_o and occluded P pools along our climosequence supports the application of the Walker and Syers [1976] model to arid and semi-arid ecosystems, not just across chronosequences but also along climosequences.

The concentration of P_{Ca} generally declined with decreasing aridity, except for three relatively higher values in the wettest sites, which may be outliers due to their relatively low sand contents (Fig. S2). The general decline of the P_{Ca} pool with decreasing aridity agrees with the prediction of the Walker and Syers [1976] model and the findings of many previous studies that examined the primary stages of soil genesis [e.g., *Syers and Walker*, 1969a; *Ippolito et al.*, 2010; *Selmants and Hart*, 2010]. The decline of P_{Ca} corresponds with a marked decline in soil exchangeable Ca in our climosequence [*Luo*, 2015], suggesting enhanced leaching of P_{Ca} along with weatherable cations. This is consistent with results from previous studies along chronosequences in humid and Mediterranean ecosystems, in which P_{Ca} declined rapidly during the initial stages of soil development [*Syers and Walker*, 1969a; *Walker and Syers*, 1976; *Richardson et al.*, 2004; *Turner and Laliberté*, 2015]. However, P_{Ca} still constituted about 30% of the P_t in the wettest soils along our climosequence, in contrast to similar-aged soils in humid ecosystems, such as tropical forests in New Zealand and Hawaii, where P_{Ca} is exhausted after approximately 10,000 years of pedogenesis [*Walker and*

Syers, 1976; *Crews et al.*, 1995]. This reflects the fact that the wettest sites in our study receive only about 400 mm of annual precipitation, which has been insufficient to completely deplete the soil of P_{Ca}. The pattern of P_{Ca} along the climosequence supports the prediction of Walker and Syers [1976] that P transformation are slower in arid sites with low leaching intensity, and suggests that soils along our climosequence are still pedogenically immature.

Occluded P and P_o that is mostly associated with Al and Fe oxides (NaOH-P_o, the main P_o fraction, Fig. S2) gradually increased along the climosequence, both in absolute terms and as a fraction of P_t (Fig. 4c, d; Fig. 5), as has been widely demonstrated by chronosequence studies of the early stages of soil development [*Syers and Walker*, 1969b; *Walker and Syers*, 1976; *Lajtha and Schlesinger*, 1988; *Ippolito et al.*, 2010]. Along our climosequence, greater P_o concentrations are associated with increasing biomass production (i.e. ANPP and MBC) [*Wang et al.*, 2014] and greater associated P inputs as organic residues along the climosequence [*Cross and Schlesinger*, 1995; 2001; *Ippolito et al.*, 2010]. Moreover, we observed significant positive correlations between extracted P_o and exchangeable Fe and Mn (Table 1), suggesting that the high specific surface areas are of these metal oxides [*Luo*, 2015] sorb and stabilize P_o in the soil [*Celi et al.*, 1999; *Turner et al.*, 2002]. Further, P_o and MAT were negatively correlated along the transect (Fig. S3), suggesting that low temperatures might also contribute to the accumulation of P_o in wetter sites through reduced microbial activity [*Post et al.*, 1985; *Zheng et al.*, 2009; *Wang et al.*, 2014]. In weakly and moderately weathered soils, occluded P is mostly recalcitrant P_o [*Williams et al.*, 1967; *Walker and Syers*, 1976], suggesting that the increase in occluded P with pedogenesis might be related to the increase in total P_o with decreasing aridity.

A notable difference between our results and the Walker and Syers [1976] model is the behavior of P_t, which should decrease continuously with increasing pedogenesis [*Walker and Syers*, 1976]. Along the climosequence in this study, however, P_t decreased initially and

then increased with decreasing aridity, with the minimum concentrations at an aridity of approximately 0.70 (Fig. 2a; Fig. 4a; Fig. 5a).

We do not consider variation in parent material to be a major driver of the pattern in total P concentrations across the climosequence. In a transect of the magnitude of that studied here, there will inevitably be some variation in parent material and, therefore, in its P content. Although we do not have detailed information on this, soils across the entire 3,700 km transect were mostly derived from loess and were of similar elemental composition [*Lei et al.*, 1990; *Shi et al.*, 1990]. Moreover, data from China's second national soil survey [*NSSO*, 1998] shows that P_t concentrations in C horizons (i.e. horizons unaffected by carbonate leaching) of Haplic Calcisols, Calcic Cambisols and Calcic Kastanozems in northern China (from three typical soil profiles) were relatively similar: 590-689 mg P kg^{-1}, 480-630 mg P kg^{-1} and 550-790 mg P kg^{-1}, respectively. Collectively, these results suggest that parent material is remarkably well-constrained given the spatial extent of the transect.

Instead, we interpret the pattern of P_t along the climosequence as reflecting our focus on the surface 10 cm of soil. Surface soil should reflect patterns of P transformations during pedogenesis, as shown along chronosequences [*Richardson et al.*, 2004; *Turner et al.*, 2007; *Izquierdo et al.*, 2013]. However, in humid sites along our climoseqeunce, greater plant productivity [*Wang et al.*, 2014] will concentrate P at the surface via litter returns, counteracting the depletion of P_t from the surface by leaching [*Porder and Chadwick*, 2009]. Thus, in drier sites (aridity > 0.7), P_o concentrations are small due to water limitation of plant growth [*Wang et al.*, 2014] and P occurs mainly as P_{Ca}, resulting in decline of P_t along with P_{Ca} as aridity declines. In contrast, P_{Ca} is weathered and leached at wetter sites, but P is concentrated at the soil surface as P_o and occluded P, leading to an increase in P_t with decreasing aridity. This not only offers an explanation for the pattern of P_t observed here along the climosequence, it also indicates a marked shift in the P cycle from geochemically

dominated to biologically dominated at an aridity threshold of 0.7 – the approximate point at which the ecosystem shifts from arid to semi-arid [*UNEP*, 1992].

The pattern of non-occluded P_i along the climosequence also contrasts with results from chronosequence studies, in which labile P increased continuously in the early stages of soil development [*Walker and Syers*, 1976; *Selmants and Hart*, 2010; *Chen et al.*, 2015]. In drier sites, the decline of non-occluded P_i along the climosequence in this study might reflect decreasing concentrations of P_{Ca}, which exert a strong control on P availability in the upper horizons of calcareous soils [*Ippolito et al.*, 2010; *Emadi et al.*, 2012]. In addition, the dominant vegetation types in our drier sites are desert shrub and desert steppe, which typically support little above-ground biomass [*Pei et al.*, 2008]. Delgado-Baquerizo et al. [2013] stated that enhanced geological processes (i.e. wind erosion and photodegradation) due to low vegetation coverage in the most arid sites can promote the release of P from primary minerals, leading to a declining trend of labile P with decreasing aridity. In wetter sites, however, the increased non-occluded P_i might reflect increasing P_o mineralization, because both P_o and biological activity (i.e. ANPP and MBC) increased along the climosequence [Fig. 5a; *Wang et al.*, 2014]. Schlesinger [1991] observed faster P cycling through P_o mineralization than through rock weathering in tropical ecosystems, and indicated that P_o recycling is essential to the availability of soil P. Overall, non-occluded P_i appears to decline initially in parallel with the decline in P_{Ca} in drier sites, and then increase in parallel with the increase in P_o in wetter sites, suggesting a gradual transition of P cycling from geochemical to biological processes with soil genesis in these arid and semi-arid ecosystems.

The transition of abiotic to biotic control of P cycling is consistent with the results of Delgado-Baquerizo et al. [2013] across an aridity gradient in drylands at global scale. They stated that a difference in the response to aridity of the P cycle compared with that of C and N leads to the decoupling of C, N and P cycles (manifested as decreases of C:P and N:P) with

increasing aridity. However, Wardle [2013] commented that there was no 'decoupling' of nutrient cycles, and that the decreases of C:P and N:P with increasing aridity appear to operate in the opposite direction to pedogenesis. Our results reconcile this issue by providing evidence for an abrupt shift in pedogenic weathering status across the aridity gradient. Specifically, the 'decoupling' of nutrient cycles appears to simply reflect the influence of climate on pedogenesis. Arid conditions slow the rate of weathering, yielding pedogenically young soils with low C:P and N:P ratios (i.e., the 'decoupling' of nutrient cycles) [*Walker and Syers*, 1976; *Crews et al.*, 1995; *Turner and Laliberté*, 2015]. The increasing C:P and N:P ratios along the climosequence in this study agree with the results of long-term chronosequence studies, in which P becomes increasingly limiting compared to C and N due to the accumulation of C and N in SOM and the increasing loss of P through leaching with pedogenesis [*Walker and Syers*, 1976; *Crews et al.*, 1995; *Selmants and Hart*, 2010; *Chen et al.*, 2015; *Turner and Laliberté*, 2015]. Here, we find a distinct shift of pedogenic weathering status across the aridity gradient from dry to wet, associated with a switch in the dominant P turnover pathway from P_i to P_o along the climosequence. Should the climate become drier in these arid and semi-arid grasslands [*Gao and Giorgi*, 2008; *Feng and Fu*, 2013], shifting a site across the pedogenic threshold (aridity < 0.7), the dominant control of P cycling would shift to geochemical processes and the P cycle would become decoupled from the C and N cycles [*Delgado-Baquerizo et al.*, 2013; *Wardle*, 2013]. These results therefore provide evidence for the importance of pedogenic process in regulating the biogeochemical cycling of P and its interaction with C and N cycling in drylands [*Delgado-Baquerizo et al.*, 2013; *Wardle*, 2013], and have significant implications for predictive models of biogeochemical cycling of nutrients in drylands under global change scenarios.

5 Conclusion

The general decline in P_{Ca} and increases in P_o and occluded P in soils along this dryland climosequence are consistent with the predictions of the Walker and Syers [1976] model of soil P transformations during pedogenesis. These results indicate a progressive switch from geochemical to biological control of the P cycle as aridity declines across an aridity threshold of about 0.7. The changes in P composition occur concurrently with increasing $C:P_o$ and $N:P_o$ ratios, indicating increasing biological demand for P relative to N along the climosequence. Overall, these results suggest that the Walker and Syers [1976] model can be applied to climosequences in arid and semiarid ecosystems.

Acknowledgments and Data

This study was supported by the National Natural Science Foundation of China (41171241 and 41201290) and the Strategic Priority Research Program of the Chinese Academy of Sciences (XDB15010400). XT Lü was supported by Youth Innovation Promotion Association CAS (2014174). We wish to thank Xingguo Han, Xiaobo Wang and all the members of Shenyang sampling campaign teams from Institute of Applied Ecology, Chinese Academy of Sciences for their assistance during field sampling. We thank the anonymous reviewers for insightful comments that improved the manuscript. Data on variations of soil phosphorus fractions across the aridity gradient are provided as online supplementary material (See Figure S1). The authors declare no conflict of interest.
Correspondence and requests for materials could be addressed to Lijun Chen (ljchenchina@hotmail.com; ljchen@iae.ac.cn).

Reference

Agbenin, J., and H. Tiessen (1995), Phosphorus forms in particle-size fractions of a toposequence from northeast Brazil, *Soil Sci. Soc. Am. J.*, *59*(6), 1687-1693.

Arora, V. K. (2002), The use of the aridity index to assess climate change effect on annual runoff, *J. Hydrol.*, *265*(1), 164-177.

Aspila, K., H. Agemian, and A. Chau (1976), A semi-automated method for the determination of inorganic, organic and total phosphate in sediments, *Analyst*, *101*(1200), 187-197.

Celi, L., S. Lamacchia, F. Marsan, and E. Barberis (1999), Interaction of inositol hexaphosphate on clays: adsorption and charging phenomena, *Soil Sci.*, *164*, 574-585.

Chen, C., E. Hou, L. Condron, G. Bacon, M. Esfandbod, J. Olley, and B. Turner (2015), Soil phosphorus fractionation and nutrient dynamics along the Cooloola coastal dune chronosequence, southern Queensland, Australia, *Geoderma*, doi:10.1016/j.geoderma.2015.1004.1027.

Craine, J. M., C. Morrow, and W. D. Stock (2008), Nutrient concentration ratios and co‐limitation in South African grasslands, *New Phytol.*, *179*(3), 829-836.

Crews, T. E., K. Kitayama, J. H. Fownes, R. H. Riley, D. A. Herbert, D. Mueller-Dombois, and P. M. Vitousek (1995), Changes in soil phosphorus fractions and ecosystem dynamics across a long chronosequence in Hawaii, *Ecology*, *76*(5), 1407-1424.

Cross, A. F., and W. H. Schlesinger (1995), A literature review and evaluation of the. Hedley fractionation: Applications to the biogeochemical cycle of soil phosphorus in natural ecosystems, *Geoderma*, *64*(3), 197-214.

Cross, A. F., and W. H. Schlesinger (2001), Biological and geochemical controls on phosphorus fractions in semiarid soils, *Biogeochemistry*, *52*(2), 155-172.

Delgado-Baquerizo, M., F. T. Maestre, A. Gallardo, M. A. Bowker, M. D. Wallenstein, J. L. Quero, V. Ochoa, B. Gozalo, M. García-Gómez, and S. Soliveres (2013), Decoupling of soil nutrient cycles as a function of aridity in global drylands, *Nature*, *502*(7473), 672-676.

Emadi, M., M. Baghernejad, M. A. Bahmanyar, and A. Morovvat (2012), Changes in soil inorganic phosphorous pools along a precipitation gradient in northern Iran, *Int. J. Forest. Soil Erosi.*, *2*(3), 143-147.

FAO (1993), Global and national soils and terrain digital databases (SOTER): Procedures manual., in *World Soil Resources Reports*, edited, Food and Agriculture Organization of the United Nations, Rome, Italy.

Feng, S., and Q. Fu (2013), Expansion of global drylands under a warming climate, *Atmospheric Chemistry and Physics*, *13*(10), 081-010.

Feng, Z.-D., C. An, and H. Wang (2006), Holocene climatic and environmental changes in the arid and semi-arid areas of China: a review, *Holocene*, *16*(1), 119-130.

Gao, X., and F. Giorgi (2008), Increased aridity in the Mediterranean region under greenhouse gas forcing estimated from high resolution simulations with a regional climate model, *Global Planet Chang.*, *62*(3), 195-209.

Hance, R., and G. Anderson (1962), A comparative study of methods of estimating soil organic phosphate, *J. Soil Sci.*, *13*(2), 225-230.

Ippolito, J., S. Blecker, C. Freeman, R. McCulley, J. Blair, and E. Kelly (2010), Phosphorus biogeochemistry across a precipitation gradient in grasslands of central North America, *J. Arid Environ.*, *74*(8), 954-961.

Irwin-Williams, C., and C. V. Haynes (1970), Climatic change and early population dynamics in the southwestern United States, *Quaternary Res.*, *1*(1), 59-71.

Izquierdo, J. E., B. Z. Houlton, and T. L. V. Huysen (2013), Evidence for progressive phosphorus limitation over long-term ecosystem development: Examination of a biogeochemical paradigm, *Plant Soil*, *367*(1-2), 135-147.

Khormali, F., and M. Kehl (2011), Micromorphology and development of loess-derived surface and buried soils along a precipitation gradient in Northern Iran, *Quatern. Int.*, *234*(1), 109-123.

Lajtha, K., and W. H. Schlesinger (1988), The biogeochemistry of phosphorus cycling and phosphorus availability along a desert soil chronosequence, *Ecology*, *69*(1), 24-39.

Lei, W., R. Huang, and J. Li (1990), Desert soils, in *Soils of China*, edited by C. Li and O. Sun, pp. 173-190, Science Press, Beijing, China.

Liangwu, L., and M. Angjiang (2001), Radiocarbon ages of soils in China, *Acta Pedo. Sinica.*, *38*(4), 513-520.

Luo, W. (2015), Zonal differentiation of elements in soil-plant system across Northern China's grasslands. PhD Dissertation, 61-93 pp, University of Chinese Academy of Sciences, Shenyang.

Luo, W., F. A. Dijkstra, E. Bai, J. Feng, X.-T. Lü, C. Wang, H. Wu, M.-H. Li, X. Han, and Y. Jiang (2016), A threshold reveals decoupled relationship of sulfur with carbon and

nitrogen in soils across arid and semi-arid grasslands in northern China, *Biogeochemistry*, *127*(1), 141-153.

Luo, W. T., J. J. Elser, X. T. Lu, Z. W. Wang, E. Bai, C. F. Yan, C. Wang, M. H. Li, N. E. Zimmermann, X. G. Han, Z. W. Xu, H. Li, Y. N. Wu, and Y. Jiang (2015), Plant nutrients do not covary with soil nutrients under changing climatic conditions, *Global Biogeochem. Cy.*, *29*(8), 1298-1308.

Mackenzie, F. T., L. M. Ver, and A. Lerman (2002), Century-scale nitrogen and phosphorus controls of the carbon cycle, *Chem. Geol.*, *190*(1), 13-32.

McGroddy, M. E., W. L. Silver, R. C. Oliveira, W. Z. Mello, and M. Keller (2008), Retention of phosphorus in highly weathered soils under a lowland Amazonian forest ecosystem, *J. Geophys. Res-Biogeo.*, *113*(G4), 608-615.

NSSO (1998), *National Soil Survey Office , Soil of China*, China Agriculture Press, Beijing.

Okin, G. S., N. Mahowald, O. A. Chadwick, and P. Artaxo (2004), Impact of desert dust on the biogeochemistry of phosphorus in terrestrial ecosystems, *Global Biogeochem. Cy.*, *18*(2), 649-655.

Pei, S. F., H. Fu, and C. G. Wan (2008), Changes in soil properties and vegetation following exclosure and grazing in degraded Alxa desert steppe of Inner Mongolia, China, *Agr. Ecosyst. Environ.*, *124*(1-2), 33-39.

Porder, S., and O. A. Chadwick (2009), Climate and soil-age constraints on nutrient uplift and retention by plants, *Ecology*, *90*(3), 623-636.

Post, W. M., J. Pastor, P. J. Zinke, and A. G. Stangenberger (1985), Global patterns of soil nitrogen storage, *Nature*, *317*(6038), 613-616.

Quénard, L., A. Samouëlian, B. Laroche, and S. Cornu (2011), Lessivage as a major process of soil formation: a revisitation of existing data, *Geoderma*, *167*, 135-147.

Richardson, S. J., D. A. Peltzer, R. B. Allen, M. S. McGlone, and R. L. Parfitt (2004), Rapid development of phosphorus limitation in temperate rainforest along the Franz Josef soil chronosequence, *Oecologia*, *139*(2), 267-276.

Roberts, T., J. Stewart, and J. Bettany (1985), The influence of topography on the distribution of organic and inorganic soil phosphorus across a narrow environmental gradient, *Can. J. Soil Sci.*, *65*(4), 651-665.

Schlesinger, W. (1991), *Biogeochemistry: An analysis of global change*, Academic Press, San Diego, CA.

Selmants, P. C., and S. C. Hart (2010), Phosphorus and soil development: does the Walker and Syers model apply to semiarid ecosystems?, *Ecology*, *91*(2), 474-484.

Shi, Y., W. Cai, and Y. Gao (1990), Castanozems, brown pedocals and sierozems, in *Soils of China*, edited by C. Li and O. Sun, pp. 154-167, Science Press, Beijing, China.

Syers, J. K., and T. W. Walker (1969a), Phosphorus transformations in a chronosequence of soils development on wind-blown sand in New Zealand.:II. Inorganic phosphorus, *J. Soil Sci.*, *20*(2), 318-324.

Syers, J. K., and T. W. Walker (1969b), Phosphorus transformations in a chronosequence of soils development on wind-blown sand in New Zealand.: I. Total and organic phosphorus, *J. Soil Sci.*, *20*(1), 57-64.

Tiessen, H., and J. Moir (1993), Characterization of available P by sequential extraction, in *Soil sampling and methods of analysis*, edited by M. R. Carter, pp. 5-229, Lewis Publishers, Ann Arbor.

Tiessen, H., J. Stewart, and C. Cole (1984), Pathways of phosphorus transformations in soils of differing pedogenesis, *Soil Sci. Soc. Am. J.*, *48*(4), 853-858.

Turner, B. L., and L. M. Condron (2013), Pedogenesis, nutrient dynamics, and ecosystem development: the legacy of TW Walker and JK Syers, *Plant Soil*, *367*(1-2), 1-10.

Turner, B. L., and E. Laliberté (2015), Soil Development and Nutrient Availability Along a 2 Million-Year Coastal Dune Chronosequence Under Species-Rich Mediterranean Shrubland in Southwestern Australia, *Ecosystems*, *18*(2), 1-23.

Turner, B. L., M. J. Papházy, P. M. Haygarth, and I. D. McKelvie (2002), Inositol phosphates in the environment, *Philos. T. Royal. Soc. B: Biol. Sci.*, *357*(1420), 449-469.

Turner, B. L., L. M. Condron, S. J. Richardson, D. A. Peltzer, and V. J. Allison (2007), Soil organic phosphorus transformations during pedogenesis, *Ecosystems*, *10*(7), 1166-1181.

UNEP (1992), World atlas of desertification edited, Edward Arnold, Seven Oaks, Nairobi, Kenya.

Vitousek, P. M., and H. Farrington (1997), Nutrient limitation and soil development: experimental test of a biogeochemical theory, *Biogeochemistry*, *37*(1), 63-75.

Vitousek, P. M., S. Porder, B. Z. Houlton, and O. A. Chadwick (2010), Terrestrial phosphorus limitation: mechanisms, implications, and nitrogen-phosphorus interactions, *Ecol. Appl.*, *20*(1), 5-15.

Walker, T. (1965), The significance of phosphorus in pedogenesis, in *Experimental Pedology*, edited by E. Hallsworth, pp. 295-315, Butterworths, London, U.K.

Walker, T., and A. R. Adams (1958), Studies on soil organic matter : I. influence of phosphorus content of parent materials on accumulations of carbon, notrogen, sulfer, and organic phosphorus in grassland soils, *Soil Sci.*, *85*(6), 307-318.

Walker, T., and J. Syers (1976), The fate of phosphorus during pedogenesis, *Geoderma*, *15*(1), 1-19.

Wang, C., X. Wang, D. Liu, H. Wu, X. Lü, Y. Fang, W. Cheng, W. Luo, P. Jiang, J. Shi, H. Yin, J. Zhou, X. Han, and E. Bai (2014), Aridity threshold in controlling ecosystem nitrogen cycling in arid and semi-arid grasslands, *Nat. commun.*, *5*, doi:10.1038/ncomms5799.

Wang, X. G., S. A. Sistla, X. B. Wang, X. T. Lü, and X. G. Han (2016), Carbon and nitrogen contents in particle-size fractions of topsoil along a 3000 km aridity gradient in northern China., *Biogeosciences.*, *13*, 3635-3646.

Wardle, D. A. (2013), Ecology: Drivers of decoupling in drylands, *Nature*, *502*(7473), 628-629.

Williams, J., J. K. Syers, and T. Walker (1967), Fractionation of soil inorganic phosphate by a modification of Chang and Jackson's procedure, *Soil Sci. Soc. Am. J.*, *31*(6), 736-739.

Williams, J., J. Syers, T. Walker, and R. Rex (1970), A comparison of methods for the determination of soil organic phosphorus, *Soil Sci.*, *110*(1), 13-18.

Yang, X., and W. Post (2011), Phosphorus transformations as a function of pedogenesis: A synthesis of soil phosphorus data using Hedley fractionation method, *Biogeosciences*, *8*, 2907-2916.

Zheng, Z.-M., G.-R. Yu, Y.-L. Fu, Y.-S. Wang, X.-M. Sun, and Y.-H. Wang (2009), Temperature sensitivity of soil respiration is affected by prevailing climatic conditions and soil organic carbon content: A trans-China based case study, *Soil Biol. Biochem.*, *41*(7), 1531-1540.

Zhou, G., Y. Wang, and S. Wang (2002), Responses of grassland ecosystems to precipitation and land use along the Northeast China Transect, *J. Veg. Sci.*, *13*(3), 361-368.

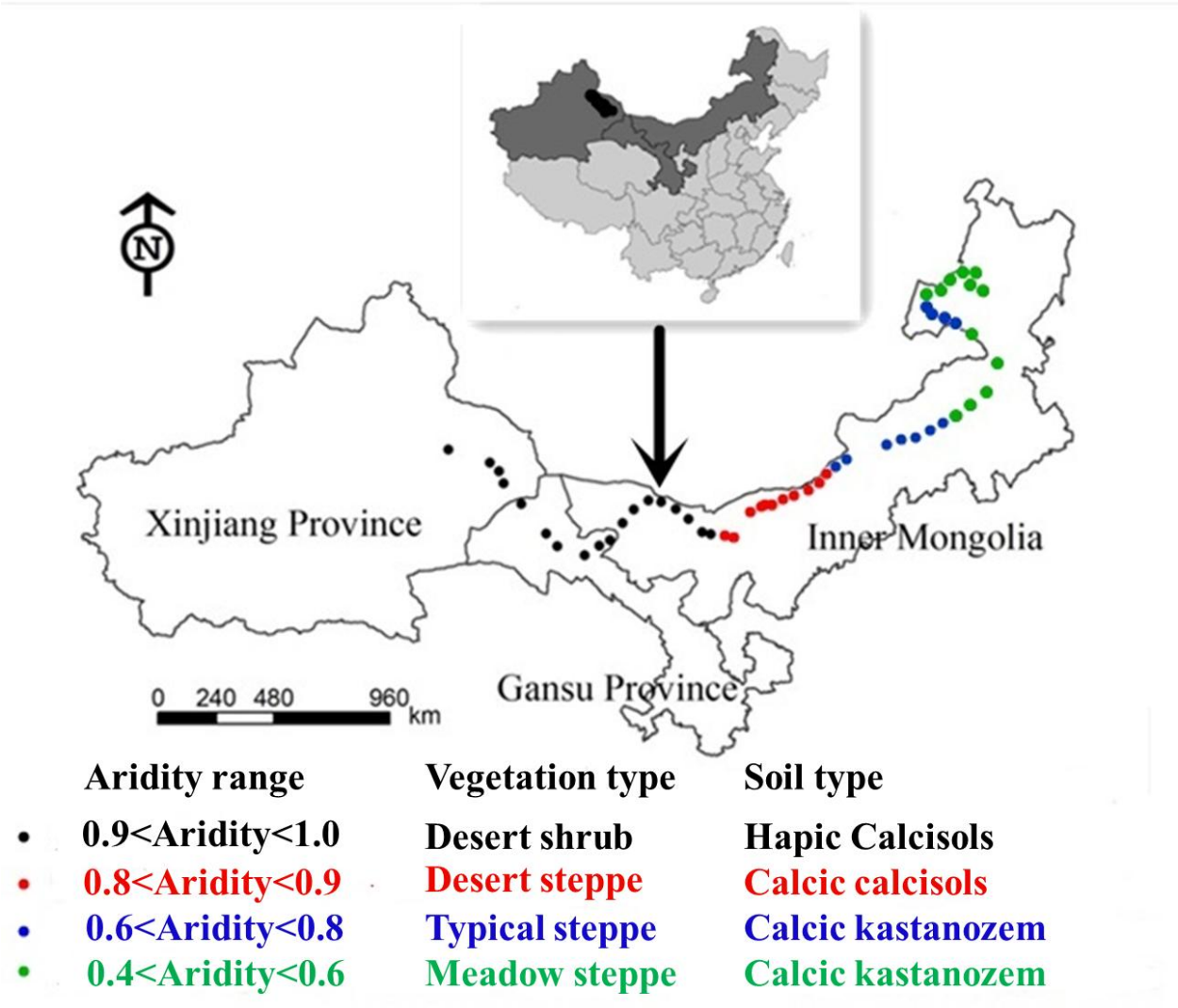

Figure 1. Geographic distribution of sample sites. Fifty-two sites were selected along a 3,700 km aridity gradient in northern China. Aridity ranged from 0.97 in the west to 0.43 in the east.

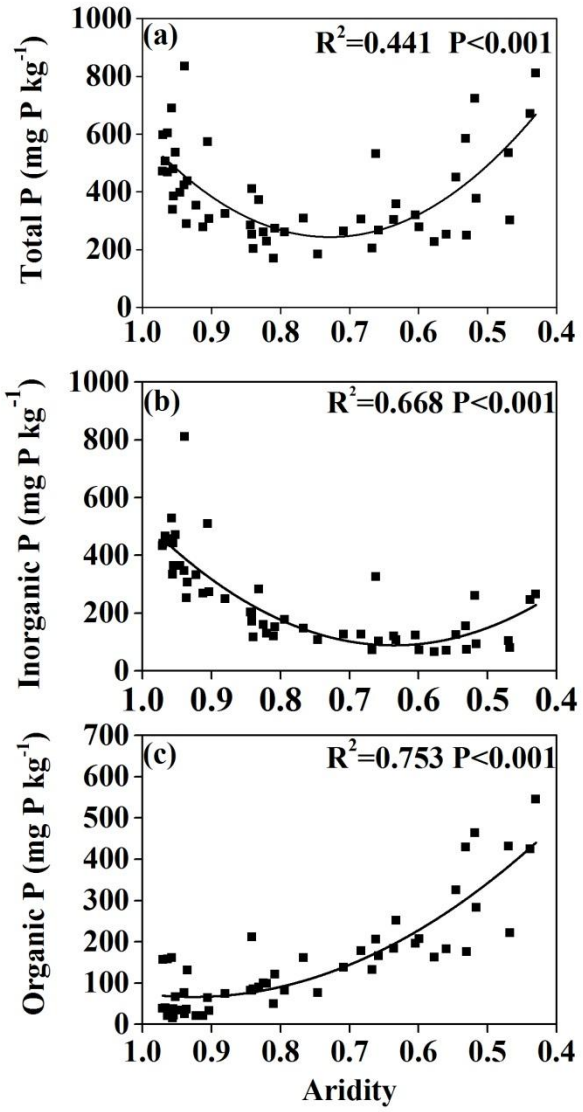

Figure 2. Soil total phosphorus, inorganic phosphorus and organic phosphorus concentrations.

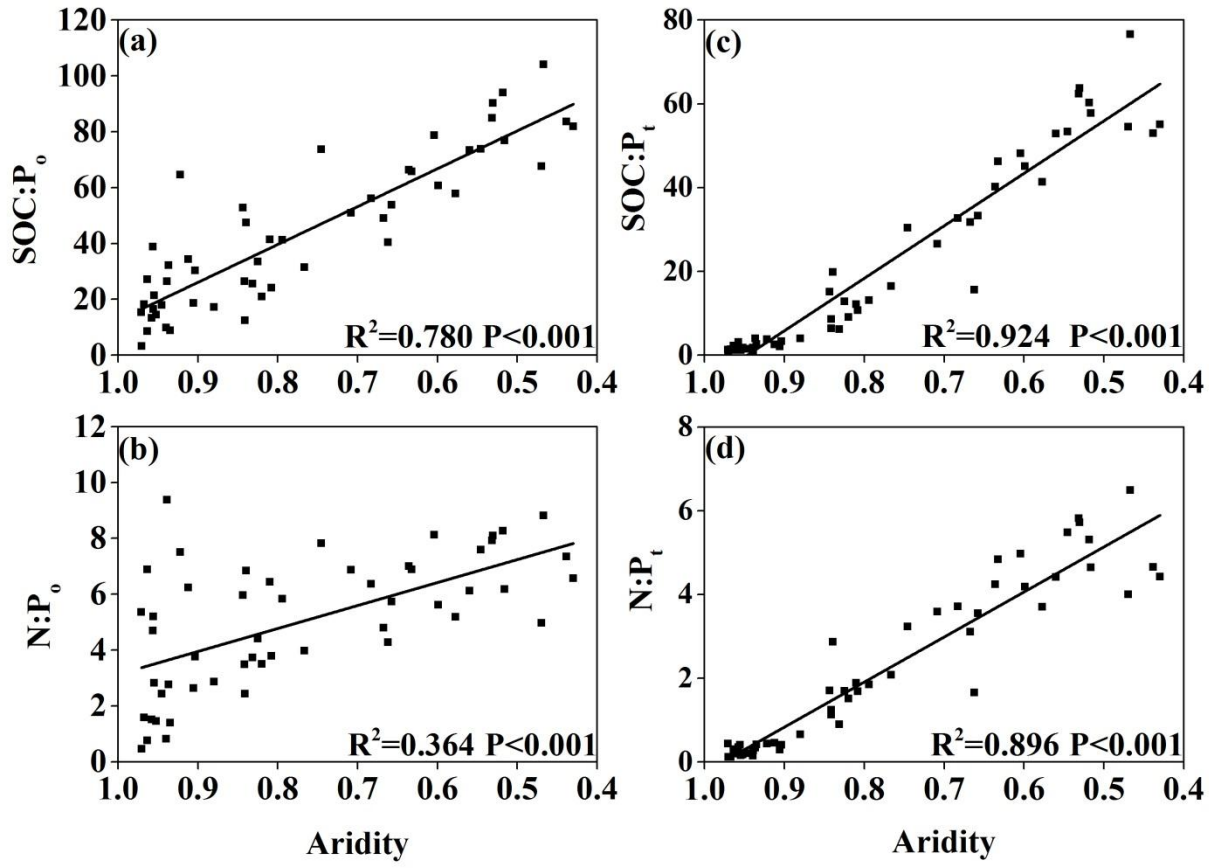

Figure 3. Soil elemental ratios (soil organic carbon, SOC; total nitrogen, N; total phosphorus, P_t; and organic phosphorus, P_o) across the aridity gradient.

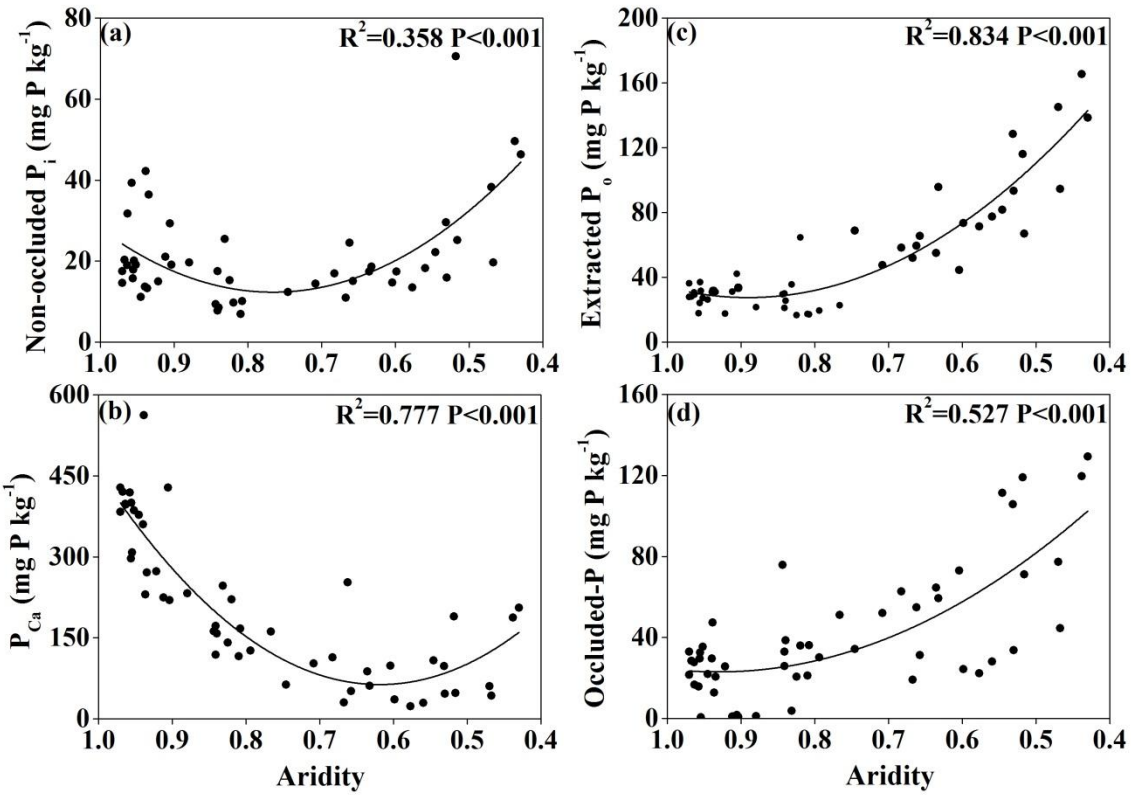

Figure 4. Changes in non-occluded P (sum of resin P, $NaHCO_3$-P_i and NaOH-P_i, mg P kg^{-1}), P_{Ca} (primary mineral P, i.e. HCl-P_i, mg P kg^{-1}), extracted P_o (sum of $NaHCO_3$-P_o, NaOH-P_o and HCl-P_o, mg P kg^{-1}) and occluded-P (residual P, mg P kg^{-1}).

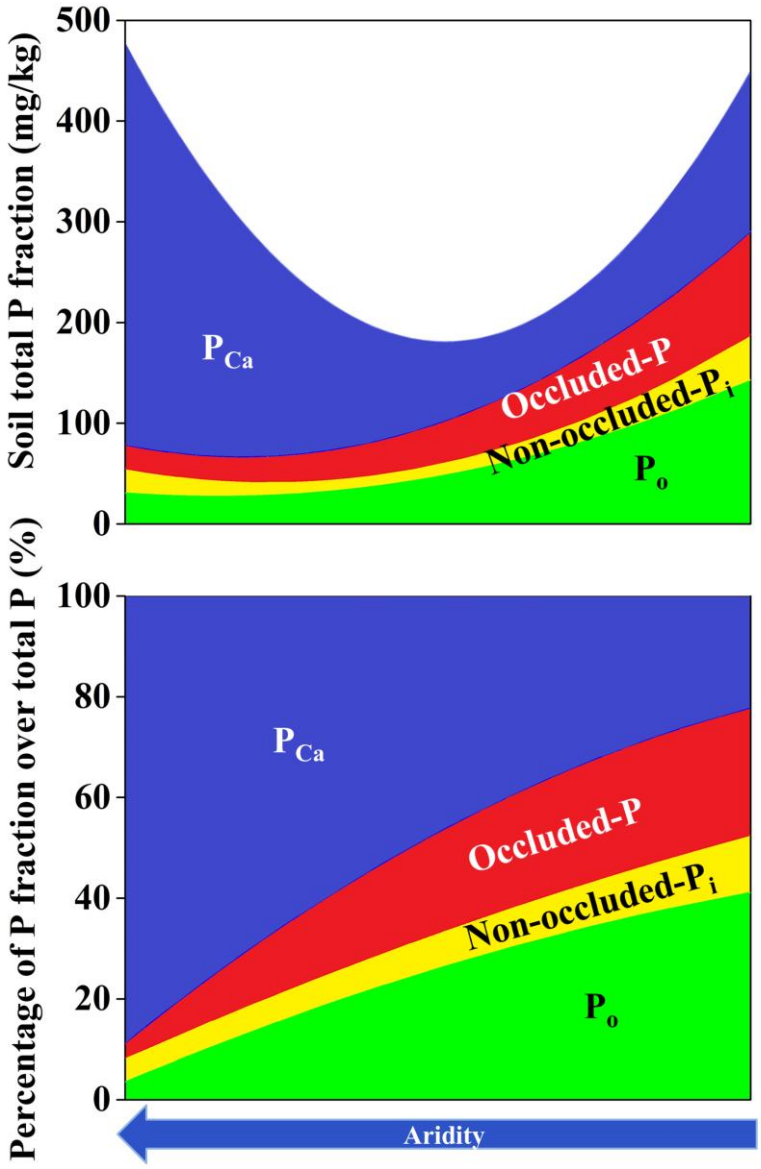

Figure 5. Panels of P fractions along the climosequence in arid and semi-arid ecosystems in northern China: the comparison to Walker and Syers diagram. (a) The amount of absolute P fraction; and (b) the percentage of P fraction in total P (%). Curves were obtained by polynomial fitting between aridity and P fractions based on 52 sample sites. P_{Ca} represents calcium phosphates in primary minerals extracted by HCl-P_i. Occluded-P represents residual-P. Non-occluded P_i is the sum of resin-P, $NaHCO_3$-P_i and NaOH-P_i. P_o is the sum of $NaHCO_3$-P_o, NaOH-P_o, HCl-P_o.

Table 1.

Pearson correlation coefficients among key soil chemical properties and concentrations (mg P kg^{-1}) of phosphorus fractions in soils along the grassland transect in northern China.

	P_t	P_i	Extracted P_o	Available-P_i	NaOH-P_i	HCl-P_i	$NaHCO_3$-P_o	NaOH-P_o	HCl-P_o	Residual P
pH	ns	0.535*	-0.834**	ns	-0.787**	0.575**	ns	-0.861**	ns	-0.631**
Ca^{2+}	0.537**	0.641**	-0.348*	ns	-0.337*	0.651**	ns	-0.340*	ns	ns
Fe^{2+}	ns	ns	0.770**	0.487**	0.855**	ns	ns	0.823**	ns	0.663**
Mn^{2+}	ns	ns	0.822**	0.488**	0.905**	-0.295*	ns	0.847**	ns	0.750**

* indicates $p<0.05$ and ** $p<0.01$ (n=52). ns, not significant.

Available-P_i, sum of resin-P and $NaHCO_3$-P_i. P_i, sum of available-P_i, NaOH-P_i and HCl-P_i. Extracted P_o, sum of $NaHCO_3$-P_o, NaOH-P_o and HCl-P_o. P_t, sum of P_i, P_o and residual P.